Inorg. Chem. **2005**, *44*, 1904–1913

A Computational and Experimental Study of the Structures and Raman and ^{77}Se NMR Spectra of SeX_3^+ and SeX_2 (X = Cl, Br, I): FT-Raman Spectrum of $(SeI_3)[AsF_6]$

J. Mikko Rautiainen,[†] Todd Way,[§] Gabriele Schatte,[§] Jack Passmore,*[,§] Risto S. Laitinen,*[,‡] Reijo J. Suontamo,[†] and Jussi Valkonen[†]

Department of Chemistry, University of Jyväskylä, P.O. Box 35, FIN-40014, Finland, Department of Chemistry, University of New Brunswick, Fredericton, New Brunswick E3B 6E2, Canada, and Department of Chemistry, University of Oulu, P.O. Box 3000, FIN-90014, Finland

Received December 1, 2004

The ability of MP2, B3PW91 and PBE0 methods to produce reliable predictions in structural and spectroscopic properties of small selenium–halogen molecules and cations has been demonstrated by using 6-311G(d) and cc-pVTZ basis sets. Optimized structures and vibrational frequencies agree closely with the experimental information, where available. Raman intensities are also well reproduced at all levels of theory. Calculated GIAO isotropic shielding tensors yield a reasonable linear correlation with the experimental chemical shift data at each level of theory. The largest deviations between calculated and experimental chemical shifts are found for selenium–iodine species. The agreement between observed and calculated chemical shifts for selenium–iodine species can be improved by inclusion of relativistic effects using the ZORA method. The best results are achieved by adding spin–orbit correction terms from ZORA calculations to nonrelativistic GIAO isotropic shielding tensors. The calculated isotropic shielding tensors can be utilized in the spectroscopic assignment of the ^{77}Se chemical shifts of novel selenium–halogen molecules and cations. The experimental FT-Raman spectra of $(SeI_3)[AsF_6]$ in the solid state and in SO_2(l) solution are also reported.

Introduction

Selenium chlorides and bromides SeX_4 and Se_2X_2 (X = Cl, Br) are well-characterized compounds and form a useful class of reagents for many synthetic applications.[1] It is also well-established that thermal decomposition of Se_2Cl_2 and Se_2Br_2 leads to the formation of $SeCl_2$ and $SeBr_2$ in the gas phase. Both dihalides can be stabilized in coordinating solvents such as thf,[2] and solid tetrahydrothiophene[2] and triphenylphosphine[3] adducts of $SeCl_2$, as well as tetramethylthiourea adducts of $SeCl_2$ and $SeBr_2$ [2,4] have been structurally characterized.

By contrast, it has not been possible to isolate and characterize SeI_4, Se_2I_2, and other electrically neutral selenium−iodine compounds,[1] though there is spectroscopic evidence of the presence of SeI_2 and Se_2I_2 in CS_2 solution.[5] The chemistry of selenium−iodine cations, on the other hand, has seen rapid progress in recent years.[6]

The simplest solid selenium−iodine cation that has been characterized in the solid state by X-ray crystallography is

* Authors to whom correspondence should be addressed. Tel.: (1506) 453-4821. Fax: (1506) 453-4981. E-mail: passmore@unb.ca (J.P.); Tel.: (3588) 553-1611. Fax: (3588) 553-1608. E-mail: risto.laitinen@oulu.fi (R.S.L.).

[†] University of Jyväskylä.

[‡] University of Oulu.

[§] University of New Brunswick.

(1) Krebs, B.; Ahlers, F.-P. *Adv. Inorg. Chem.* **1990**, *35*, 235. (b) Behrendt, U.; Gerwarth, U. W.; Jager, S.; Kreuzbichzer, I.; Seppelt, K. *Gmelin's Handbook of Inorganic Chemistry*, 8th ed.; Springer-Verlag: Berlin, 1984; Selenium Suppl. Vol. B2.

(2) Maaninen, A.; Chivers, T.; Parvez, M.; Pietikäinen, J.; Laitinen, R. S. *Inorg. Chem.* **1999**, *38*, 4093.

(3) For preliminary information on the preparation, structural characterization, and bonding of $(Ph_3PO)_2SeCl_2$, see: Suontamo, R.; Maaninen, A.; Laitinen, R. S.; Chivers, T. Canadian Society for Chemistry Conference and Exhibition, Calgary, Canada, 27.-31.5.2000. paper no. IN435.

(4) Wynne, K. J.; Pearson, P. S.; Newton, M. G.; Golen, J. *Inorg. Chem.* **1972**, *11*, 1192.

(5) Gopal, M.; Milne, J. *Inorg. Chem.* **1992**, *31*, 4530.

(6) (a) Klapötke, T.; Passmore, J. *Acc. Chem. Res.* **1989**, *22*, 234. (b) Chemistry of Inorganic Ring Systems. In *Studies in Inorganic Chemistry*; Passmore, J., Steudel, R., Ed.; Elsevier: Amsterdam, 1992; p 373.

10.1021/ic048310w CCC: $30.25
Published on Web 02/23/2005

the pyramidal SeI_3^+ cation.[7] Its chlorine and bromine analogues are also known.[8] Other well-characterized selenium−iodine cations comprise $Se_2I_4^{2+}$,[9] $Se_4I_4^{2+}$,[10] $(Se_6I^+)_n$,[11] and $Se_6I_2^{2+}$.[11b,12] In the solid state they adopt polymeric, ring, and cage structures.[6]

In SO_2 solution these cations are involved in complicated equilibria.[6] This is clearly demonstrated by $(Se_6I_2)[MF_6]_2$ (M = As) the dissociation of which has been investigated by ^{77}Se NMR spectroscopy at −80 °C in SO_2(l) using both natural-abundance and ^{77}Se-enriched selenium (enrichment 92.4%).[13] The spectrum of the equilibrium mixture was found to contain eleven cations the spin systems of which have been identified using ^{77}Se-^{77}Se COSY, selective irradiation experiments, and spectral simulation. Combination of this information with the trends in the chemical shifts as well as the consideration of iodine, selenium, and charge balances that were calculated from the integrated intensities resulted in the suggestion of the chemical identities of the actual cations present in the solution. The formation of such equilibria is believed to be entropy-driven, since enthalpies of different compounds are close to each other.[6]

The unambiguous identification of components in the complicated mixtures of selenium−iodine cations cannot rely on experimental spectroscopic information alone. The interpretation of NMR and vibrational spectra necessitates computational methods for the modeling of structures and spectroscopic properties. The reliability of the computational approach is dependent on the method, level of theory, inclusion of electron correlation, and the consideration of relativistic effects.

Although good results have been reported for some selenium compounds with ab initio RHF and MP2 methods,[14] these methods fail to reproduce consistently the experimental properties of the cationic selenium species. For example, the experimental geometry of Se_8^{2+} was not satisfactorily predicted by RHF/6-311G* and MP2/6-311G* calculations.[15] Only the more recent B3PW91/6-311G(2df) and MPW1PW91/6-311G(2df) optimized structures were in good agreement with experiment.[16] Another example of the inability of RHF and MP2 methods to model the properties of selenium cations involves the GIAO RHF/6-41+G*//MP2/6-41G* and MP2/6-41+G*//MP2/6−41G* calculations of ^{77}Se NMR chemical shift of Se_4^{2+} that yielded the values 3821 and 154 ppm, respectively[14b] (cf. the experimental value of 1936 ppm[17]).

GIAO DFT computations on Se_4^{2+} are in better agreement with experiment. Schrechenbach et al.[18] calculated the chemical shift of 1834 ppm using the PB86 functional. Tuononen et al.[19] used the BPW91 and B3PW91 functionals and obtained chemical shifts of 1941 and 2120 ppm, respectively. They reported that the problems with single reference ab initio methods were due to the singlet diradical nature of Se_4^{2+}. This inference was supported by the multireference [22,16]-CAS calculations yielding the ^{77}Se chemical shift of 1893 ppm for Se_4^{2+} that is in reasonable agreement with the experimental value.[19]

While chemical shifts of several selenium compounds can be calculated with good accuracy by using nonrelativistic methods,[18,20] considerations of relativistic effects and spin−orbit corrections on the ^{77}Se chemical shift become important, when selenium is bound to iodine or another 5th row atom in the Periodic Table. Especially spin−orbit contribution has been shown to have a major effect on the shielding tensors of lighter nuclei in molecules containing heavy halogen atoms.[21]

The fully relativistic four-component calculations are computationally very demanding. Therefore for large systems of chemical interest it is more attractive to evaluate the relativistic effects by utilizing two-component approximations.[22] One of the successful approximations that have been applied for the relativistic chemical shift calculations is the ZORA NMR method.[23,24] Other methods for estimating relativistic NMR parameters have also been reported,[25] but to our knowledge they are not yet generally available. The inclusion of scalar relativistic effects by using quasi-

(7) Johnson, J. P.; Murchie, M.; Passmore, J.; Tajik, M.; White, P. S.; Wong, C.-M. *Can. J. Chem.* **1987**, *65*, 2744.
(8) (a) Passmore, J.; Cameron, T. S.; Boyle, P. D.; Schatte, G.; Way, T. *Can. J. Chem.* **1996**, *74*, 1671. (b) Passmore, J.; Richardson, E. K.; Whidden, T. K.; White, P. S. *Can. J. Chem.* **1980**, *58*, 851. (c) Brooks, W. V. F.; Passmore, J.; Richardson, E. K. *Can. J. Chem.* **1979**, *57*, 3230.
(9) Nandana, W. A. S.; Passmore, J.; White, P. S.; Wong, C.-M. *Inorg. Chem.* **1990**, *29*, 3529.
(10) Carnell, M. M.; Grein, F.; Murchie, M.; Passmore, J.; Wong, C.-M. *J. Chem. Soc., Chem. Commun.* **1986**, 225−7.
(11) (a) Nandana, W. A. S.; Passmore, J.; White, P. S. *J. Chem. Soc., Chem. Commun.* **1983**, 526. (b) Nandana, W. A. S.; Passmore, J.; White, P. S.; Wong, C.-M. *Inorg. Chem.* **1989**, *28*, 3320.
(12) Passmore, J.; White, P. S.; Wong, C.-M. *J. Chem. Soc., Chem. Commun.* **1985**, 1178.
(13) Brownridge, S.; Calhoun, L.; Laitinen, R. S.; Passmore, J.; Pietikäinen, J.; Saunders: J. *Phosphorus, Sulfur Silicon Relat. Elem.* **2001**, *168*−*169*, 105.
(14) (a) Suontamo, R. J.; Laitinen, R. S. *Main Group Chem.* **1996**, 1, 241. (b) Bühl, M.; Thiel, W.; Fleischer, U.; Kutzelnigg, W. *J. Phys. Chem.* **1995**, *99*, 4000. (c) Suontamo, R. J.; Laitinen, R. S. *J. Mol. Struct. (THEOCHEM)* **1995**, *336*, 55. (d) Broschag, M.; Klapötke, T. M.; Schulz, A.; White, P. S. *Inorg. Chem.* **1993**, *32*, 5734.; (e) Magyarfalvi, G.; Pulay, P. *Chem. Phys. Lett.* **1994**, *225*, 280.
(15) Cioslowski, J.; Gao, X. *Int. J. Quantum. Chem.* **1997**, *65*. 609.
(16) Cameron, T. S.; Deeth, R. J.; Dionne, I.; Du, H.; Jenkins, H. D. B.; Krossing, I.; Passmore, J.; Roobottom, H. K. *Inorg. Chem.* **2000**, *39*, 5614.
(17) Collins, M. J.; Gillespie, R. J.; Sawyer, J. F.; Schrobilgen, G. J. *Inorg. Chem.* **1986**, *25*, 2053.
(18) Schreckenbach, G.; Ruiz-Morales, Y.; Ziegler, T. *J. Chem. Phys.* **1996**, *104*, 8605.
(19) Tuononen, H. M.; Suontamo, R. S.; Valkonen, J.; Laitinen, R. S. *J. Phys. Chem. A* **2004**, *108*, 5670.
(20) (a) Bayse, C. A. *Inorg. Chem.* **2004**, *43*, 1208. (b) Nakanishi, W.; Hayashi, S. *J. Phys. Chem. A* **1999**, *103*, 6074. (c) Maaninen, T.; Tuononen, H. M.; Kosunen, K.; Oilunkaniemi, R.; Hiitola, J.; Laitinen, R. S.; Chivers, T. *Z. Anorg. Allg. Chem.* **2004**, *630*, 1947.
(21) Kaupp, M.; Malkin, V. G.; Malkina, O. L.; Pyykkö, P. *Chem. Eur. J.* **1998**, *4*, 118.
(22) (a) van Lenthe, E.; Baerends, E. J.; Snijder, J. G. *J. Chem. Phys.* **1993**, *99*, 4597. (b) Douglas, M.; Kroll, N. M. *Ann. Phys.* **1974**, *82*, 89. (c) Dyall, K. G. *J. Chem. Phys.* **1997**, *106*, 9618.
(23) Wolff, S. K.; Ziegler, T.; van Lenthe, E.; Baerends, E. J. *J. Chem. Phys.* **1999**, *110*, 7689.
(24) (a) Bouten, R.; Baerends, E. J.; van Lenthe, E.; Visscher, L.; Schreckenbach, G.; Ziegler, T. *J. Phys. Chem. A* **2000**, *104*, 5600. (b) Schreckenbach, G. *Inorg. Chem.* **2002**, *41*, 6560. (c) Bagno, A.; Rastrelli, F.; Saielli, G. *J. Phys. Chem. A* **2003**, *107*, 9964.
(25) (a) Fukuda, R.; Hada, M.; Nakatsuji, H. *J. Chem. Phys.* **2003**, *118*, 1015. (b) Baba, T.; Fukui, H. *Mol. Phys.* **2002**, *100*, 623. (c) Fukui, H.; Baba, T.; Shiraishi, Y.; Imanishi, S.; Kudo, K.; Mori, K.; Shimoji, M. *Mol. Phys.* **2004**, *102*, 641. (d) Yates, J. R.; Pickard, C. J.; Payne, M. C.; Mauri, F. *J. Chem. Phys.* **2003**, *118*, 5746.

relativistic effective core potential (ECP) basis sets is an attractive approach because of their ready availability and computational efficiency. They have been shown to provide good approximations for the geometries and vibrational frequencies of small selenium-containing molecules,[26] and it has been suggested that in case of closely related molecules the linear correlation between chemical shielding tensors from ECP basis set calculations and experimental chemical shifts would allow their use in the identification of unknown members in these homologous series.[27] It is, however, generally considered that the use of ECP basis sets should be avoided on the atom for which the NMR parameters are calculated, because NMR parameters depend critically on the shape of the molecular orbitals near the nucleus.[28] With the ECP basis sets molecular orbitals decrease monotonically to zero at distances shorter than core radius and are thus not correctly modeled near nucleus.[28b] Therefore we have restricted the use of ECP basis set only on iodine atoms and used all electron basis sets for all other elements.

A compromise between the accuracy and the computational resources is necessary in case of large molecular systems involving heavy atoms. Since the multireference CAS calculations are computationally very demanding, it seems that the density functional methods would be an efficient choice for the calculations. We have chosen to utilize the B3PW91 hybrid functional that was used by Tuononen et al.[19] and the newer PBE0 hybrid functional in our calculations. The MP2 method is also used as a reference to evaluate the performance of the two density functionals.

The goal of the present study is to find an accurate and computationally efficient method for calculation of the vibrational and ^{77}Se NMR spectroscopic properties for small selenium−halogen molecules and cations. The computational results for SeX_2 (X = Cl, Br, I) molecules are compared with the experimental data, where available.[2,29] The experimental information for the SeX_3^+ (X = Cl, Br, I) cations is taken from the AsF_6^- salts, since the use of a nonbasic anion minimizes the electronic interactions with these electrophilic cations and enables direct comparison with the computational gas-phase data in a consistent manner.[7,8] FT-Raman spectra are known for $(SeCl_3)[MF_6](s)$ and $(SeBr_3)[MF_6](s)$ (M = As, Sb).[8] In this contribution we report the FT-Raman spectrum of $(SeI_3)[AsF_6]$ both in solid state and in $SO_2(l)$ solution. The reference compounds in isotropic shielding tensor calculations include also SeR_2 (R = H and Me),[30] Se_2X_2 (X = Cl, Br, Me), Se_6 and Se_8 molecules for which unambiguous experimental NMR data are available.[31] The shielding tensor calculations also verify the correct assignment of the ^{77}Se NMR resonance at 918 ppm to Se_2I_2.[5]

Computational Details

All geometry optimizations and frequency calculations were performed with the *Gaussian* 98 program package[32] at MP2 and hybrid DFT levels of theory. DFT calculations employed Becke's three-parameter hybrid functional combined with the Perdew/Wang 91 correlation functional (B3PW91)[33] and the hybrid PBE0 functional which is a modification of the original gradient corrected exchange-correlation functional by Perdew, Burke and Ernzerhof.[34] Pople-type 6-311G(d)[35] and Dunning's correlation consistent cc-pVTZ[36] basis sets were utilized in hybrid DFT and MP2 calculations. SDB-cc-pVTZ[37] effective large core potential basis set was used for iodine atoms in cc-pVTZ calculations.

Full geometry optimizations for the SeX_3^+ cations were performed by constraining the species in C_{3v} symmetry. Those for the Se_2X_2 and Se_2Me_2 molecules were carried out in C_2 symmetry, that for Se_6 in D_{3d} symmetry, that for Se_8 in D_{4d} symmetry, and those for SeX_2 (X = Cl, Br, I), SeH_2 and $SeMe_2$ molecules in C_{2v} symmetry. Since the shielding tensor of $SeMe_2$ has been shown to depend on the conformation of the molecule,[38] we adopted that of the staggered−staggered conformation for a chemical shift reference point in a similar manner.

(26) (a) El-Azhary, A. A.; Al-Kahtani, A. A. *J. Mol. Struct. (THEOCHEM)* **2001**, *572*, 81. (b) Ribeiro-Claro, P. J. A.; Amado, A. M. *J. Mol. Struct. (THEOCHEM)* **2000**, *528*, 19.

(27) (a) Komulainen, J.; Laitinen, R. S.; Suontamo, R. J. *Can. J. Chem.* **2002**, *80*, 1435. (b) Bagno, A.; Bonchio, M. *Chem. Phys. Lett.* **2000**, *317*, 123.

(28) (a) Helgaker, T.; Jaszuński, M.; Ruud, K. *Chem. Rev.* **1999**, *99*, 293. (b) Schreckenbach, G.; Ziegler, T. *Theor. Chem. Acc.* **1998**, *99*, 71.

(29) (a) Akishin, P. A.; Spiridonov, V. P.; Mishulina, R. A. *Vestn. Mosk. Univ., Ser. II, Khim.* **1962**, *17*, 23. (b) Milne, J. *Polyhedron* **1985**, *4*, 65. (c) Ozin, G. A.; Van der Voet, A. *J. Chem. Soc. D* **1970**, 896. (d) Fernholt, L.; Haaland, A.; Seip, R.; Kniep, R.; Korte, L. *Z. Naturforsch.* **1983**, *38b*, 1072.

(30) Ellis, P. D.; Odom, J. D.; Lipton, A. S.; Chen, Q.; Gulick, J. M. In *Nuclear Magnetic Shieldings and Molecular Structure*; Tossell, J. A., Ed.; NATO ASI Series, Kluwer Academics: Amsterdam, 1993; p 593.

(31) (a) Lamoureux, M.; Milne, J. *Can. J. Chem.* **1989**, *67*, 1936, and references therein. (b) Birchall, T.; Gillespie, R. J.; Vekris, S. L. *Can. J. Chem.* **1965**, *43*, 1672. (c) Christiaens, L.; Piette, J.-L.; Laitem, L.; Baiwir, M.; Denoel, J.; Llabres, G. *Org. Magn. Reson.* **1976**, *8*, 354. (d) Laitinen, R. S.; Pakkanen, T. A. *J. Chem. Soc., Chem. Commun.* **1986**, 1381. (e) Laitinen, R. S.; Pakkanen, T. A. *Inorg. Chem.* **1987**, *26*, 2598.

(32) Frisch, J. M.; Trucks, G. W.; Schlegel, H. B.; Scuseria, G. E.; Robb, M. A.; Cheeseman, J. R.; Zakrzewski, V. G.; Montgomery, J. A., Jr.; Stratmann, R. E.; Burant, J. C.; Dapprich, S.; Millam, J. M.; Daniels, A. D.; Kudin, K. N.; Strain, M. C.; Farkas, O.; Tomasi, J.; Barone, V.; Cossi, M.; Cammi, R.; Menucci, B.; Pomelli, C.; Adamo, C.; Clifford, S.; Ochterski, J.; Petersson, G. A.; Ayala, P. Y.; Cui, Q.; Morokuma, K.; Salvador, P.; Dannenberg, J. J.; Malick, D. K.; Rabuck, A. D.; Raghavachari, K.; Foresman, J. B.; Cioslowski, J.; Ortiz, J. V.; Baboul, A. G.; Stefanov, B. B.; Liu, G.; Liashenko, A.; Piskorz, P.; Komaromi, I.; Gomperts, R.; Martin, R. L.; Fox, D. J.; Keith, D. J.; Al-Laham, M. A.; Peng, C. Y.; Nanayakkara, A.; Challacombe, M.; Gill, P. M. W.; Johnson, B.; Chen, B.; Wong, M. W.; Andres, J. L.; Gonzales, C.; Head-Gordon, M.; Replogle, E. S.; Pople, J. A., Gaussian 98 (revision A.11), Gaussian, Inc., Pittsburgh, PA, 2001.

(33) (a) Becke, A. D. *J. Chem. Phys.* **1993**, *98*, 5648. (b) Perdew, J. P.; Wang, Y. *Phys. Rev. B* **1992**, *45*, 13244.

(34) (a) Perdew, J. P.; Burke, K.; Ernzerhof, M. *Phys. Rev. Lett.* **1996**, *77*, 3865; **1997**, *78*, 1396 (E). (b) Perdew, J. P.; Ernzerhof, M.; Burke, K. *J. Chem. Phys.* **1996**, *105*, 9982. (c) Adamo, C.; Barone, V. *J. Chem. Phys.* **1999**, *110*, 6158.

(35) (a) Krishnan, R.; Binkley, J. S.; Seeger, R.; Pople, J. A. *J. Chem. Phys.* **1980**, *72*, 650. (b) Blaudeau, J.-P.; McGrath, M. P.; Curtiss, L. A.; Radom, L. *J. Chem. Phys.* **1997**, *107*, 5016. (c) Curtiss, L. A.; McGrath, M. P.; Blaudeau, J.-P.; Davis, N. E.; Binning, R. C., Jr.; Radom, L. *J. Chem. Phys.* **1995**, *103*, 6104. (d) Glukhovtsev, M. N.; Pross, A.; McGrath, M. P.; Radom, L. *J. Chem. Phys.* **1995**, *103*, 1878.

(36) (a) Dunning, T. H., Jr. *J. Chem. Phys.* **1989**, *90*, 1007. (b) Woon, D. E.; Dunning, T. H., Jr. *J. Chem. Phys.* **1993**, *98*, 1358. (c) Wilson, A. K.; Woon, D. E.; Peterson, K. A.; Dunning, T. H., Jr. *J. Chem. Phys.* **1999**, *110*, 7667.

(37) (a) Martin, J. M. L.; Sundermann, A. *J. Chem. Phys.* **2001**, *114*, 3408. (b) Bergner, A.; Dolg, M.; Kuechle, W.; Stoll, H.; Preuss, H. *Mol. Phys.* **1993**, *80*, 1431.

(38) Schreckenbach, G.; Ziegler, T. *Int. J. Quantum Chem.* **1996**, *60*, 753.

Table 1. Optimized Geometries of SeX_3^+ Cations and SeX_2 Molecules (X = Cl, Br, I)

	$SeCl_3^+$ [a]		$SeBr_3^+$ [b]		SeI_3^+ [c]		$SeCl_2$ [d]		$SeBr_2$ [e]		SeI_2	
	R(Å)	∠(deg)	R(Å)	∠(deg)	R(Å)	∠(deg)	R(Å)	∠(deg)	R(Å)	∠(deg)	R(Å)	∠(deg)
MP2/cc-pVTZ	2.094	101.47	2.262	102.39	2.498	103.67	2.147	100.75	2.298	101.61	2.507	103.02
B3PW91/cc-pVTZ	2.112	102.13	2.285	103.51	2.518	105.15	2.160	101.95	2.315	103.20	2.523	104.90
PBE0/cc-pVTZ	2.102	101.89	2.275	103.22	2.507	104.79	2.151	101.61	2.305	102.79	2.513	104.42
MP2/6-311G(d)	2.117	101.62	2.285	102.72	2.538	104.10	2.173	100.87	2.322	102.05	2.544	103.46
B3PW91/6-311G(d)	2.127	102.19	2.296	103.78	2.540	105.75	2.179	101.79	2.328	103.45	2.541	105.06
PBE0/6-311G(d)	2.117	101.96	2.286	103.47	2.528	105.31	2.170	101.41	2.319	102.96	2.530	104.53
experimental	2.10	99.8	2.27	100.9	2.51	102.4	2.18	96.0	2.32	100 [f]		

[a] For experimental values, see ref 8a. [b] For experimental values, see ref 8b. [c] For experimental values, see ref 7. [d] For experimental values, see ref 29c. [e] For experimental values, see ref 29a. [f] The ∠ (Br−Se−Br) bond angle has been estimated in a vibrational spectroscopic study.[29b]

Frequency calculations were carried out for all molecules in order to establish the nature of the stationary points and to assign the experimental Raman spectra. The chemical shift calculations were carried out at a nonrelativistic level by using the Gauge-independent atomic orbital method (GIAO)[39] and at a relativistic level by using the ZORA NMR method[23,24] within the ADF program package.[40] ZORA NMR calculations employed the rPBE GGA functional[34a,41] and large QZ4P basis set, as implemented in the ADF internal basis set library.

Experimental Section

The experimental methods, equipment, and spectroscopic methods used in this work have been reported previously.[7]

The Preparation of $(SeI_3)[AsF_6]$. The preparation of $(SeI_3)[AsF_6]$ involves a minor modification of the procedure described previously.[42] The reaction flask was composed of two bulbs and a frit, as shown in the Supporting Information.

$$2Se + 3I_2 + 3AsF_5 \xrightarrow{SO_2(l)} 2SeI_3AsF_6 + AsF_3 \qquad (1)$$

Selenium (0.2322 g, 2.94 mmol) and 2.0% excess of iodine (1.1429 g, 4.50 mmol) were added into the secondary bulb of the reaction flask. SO_2 (6.4843 g, 101.3 mmol) was added into the primary bulb, followed by AsF_5 (0.7849 g, 4.61 mmol, 4.5% excess). The SO_2/AsF_5 solution was poured onto the solid Se/I_2 mixture giving an orange brown solution over a similarly colored solid. The mixture was stirred for 60 h at 20 °C followed by a slow removal of solvent yielding quantitatively black crystalline $(SeI_3)[AsF_6]$ (1.906 g, 2.94 mmol). The product was characterized by FT-Raman spectroscopy. It was found to contain trace amounts of I_2.

FT-Raman Spectra of $(SeI_3)[AsF_6]$. FT-Raman spectra both in the solid state and solution were recorded at 20 °C on a Bruker IFS-66 spectrometer equipped with a FRA-106 Raman unit and Nd:YAG laser. The data were collected in the backscattering mode (resolution 4 cm^{-1}, laser power 5 mW, 10240 scans) and corrected with the instrument response function. The crystalline sample was placed in a 5 mm NMR tube which was flame sealed before recording of the spectrum. The solution FT-Raman spectrum was recorded in situ from the orange-brown reaction solution that was poured into a 5 mm thick-walled NMR tube attached to the reaction flask.

Results and Discussion

Structures of SeX_3^+ and SeX_2 (X = Cl, Br, I). The optimized structural parameters of SeX_3^+ and SeX_2 (X = Cl, Br, I) are presented in Table 1 and compared to the experimental information where available.[43] The calculated structural parameters agree well with experimental values at each level of theory. Deviations between calculated and experimental bond lengths are less than 0.04 Å for all molecules, and the calculated bond angles are within 3 degrees of the experimental angles for all other species except $SeCl_2$. The bond angle of $SeCl_2$ is overestimated by approximately 5 degrees with all methods. MP2/cc-pVTZ calculations predict the shortest bonds and smallest bond angles, and B3PW91/6-311G(d) calculations give the longest bonds and largest bond angles. PBE0 functional gives consistently smaller bond angles and shorter bonds than the B3PW91 functional. This is an expected behavior due to the larger amount of exact exchange in the PBE0 functional.

The structural parameters of SeI_2 have been estimated at all levels of theory. The calculated Se−I bond length is 2.507−2.544 Å and the I−Se−I bond angle is 103.02−105.06°. The shortest and longest estimates for Se−I bonds are given by the MP2 calculations. DFT methods give more consistent predictions for Se−I bond lengths and are close to 2.53 Å. The smallest bond angles are predicted by MP2 calculations and the largest by B3PW91 calculations. The experimental I−Se−I bond angle is expected to be best predicted by the MP2 calculations.

Observed experimental trends are well reproduced by the optimized structural parameters. For example, the Se−I bond in SeI_2 is predicted to be longer than the corresponding bond in SeI_3^+. This is consistent with the observed trend of the Se−X bonds being longer in SeX_2 molecules than the corresponding bonds in SeX_3^+ cations in case of the lighter halogen congeners.

(39) (a) Wolinski, K.; Hilton, J. F.; Pulay, P. *J. Am. Chem. Soc.* **1990**, *112*, 8251. (b) Wolinski, K.; Sadlej, A. J. *Mol. Phys.* **1980**, *41*, 1419. (c) Ditchfield, R. *Mol. Phys.* **1974**, *27*, 789. (d) McWeeny, R. *Phys. Rev.* **1962**, *126*, 1028.

(40) (a) te Velde, G.; Bickelhaupt, F. M.; van Gisbergen, S. J. A.; Fonseca Guerra, C.; Baerends, E. J.; Snijders, J. G.; Ziegler, T. *J. Comput. Chem.* **2001**, *22*, 931. (b) Fonseca Guerra, C.; Snijders, J. G.; te Velde, G.; Baerends, E. J. *Theor. Chem. Acc.* **1998**, *99*, 391.

(41) Hammer, B.; Hansen, L. B.; Norskov, J. K. *Phys. Rev.* **1999**, *B59*, 7413.

(42) Passmore, J.; Taylor, P. *J. Chem. Soc., Dalton Trans.* **1976**, 804.

(43) All $(SeX_3)[AsF_6]$ (X = Cl, Br, I) have been structurally characterized by X-ray crystallography,[7,8] and the molecular structures of gaseous $SeCl_2$ and $SeBr_2$ have been determined by electron diffraction.[29] The X-ray structure determination of $SeCl_2 \cdot (Ph_3PO)_2$ exhibits a bent selenium dichloride molecule with similar bond parameters[3] to the molecule in the gas phase.[29c] There is no experimental information for the structure of SeI_2.[1]

Table 2. Comparison of Unscaled Calculated Vibrational Frequencies [cm^{-1}] and Relative Raman Intensities (in Parentheses) the Experimental Raman Data of SeX_3^+ and SeX_2 Molecules

	calculated							experimental		
compound	MP2/ cc-pVTZ	B3PW91/ cc-pVTZ	PBE0/ cc-pVTZ	MP2/ 6-311G(d)	B3PW91/ 6-311G(d)	PBE0/ 6-311G(d)	gas	AsF_6^-	SbF_6^-	solution
					$SeCl_3^+$[a]					
$\nu_1(A_1)$	467 (100)	447 (100)	458 (100)	443 (100)	434 (100)	445 (100)		437 (100)	433 (100)	
$\nu_2(A_1)$	213 (25)	204 (22)	208 (21)	212 (37)	204 (28)	209 (28)		207 (49)	209 (27)	
$\nu_3(E)$	458 (33)	434 (30)	446 (30)	434 (45)	421 (37)	433 (39)		418 (23)	410 (19)	
$\nu_4(E)$	170 (26)	161 (21)	164 (21)	173 (41)	164 (29)	168 (29)		176 (82)	172 (52)	
					$SeBr_3^+$[a,b]					
$\nu_1(A_1)$	314 (100)	298 (100)	304 (100)	301 (100)	294 (100)	301 (100)		292 (100)	294 (100)	291
$\nu_2(A_1)$	141 (47)	134 (41)	136 (39)	140 (70)	134 (52)	137 (51)		137 (55)	150 (95)	138
$\nu_3(E)$	327 (31)	306 (26)	314 (27)	316 (42)	304 (31)	312 (32)		292 (100)	312 (22)	298
$\nu_4(E)$	104 (37)	98 (28)	100 (27)	104 (56)	99 (36)	101 (36)		110 (85)	112 (120)	108
					SeI_3^+[c]					
$\nu_1(A_1)$	232 (100)	223 (100)	229 (100)	220 (100)	217 (100)	222 (100)		216 (100)		217 (100)
$\nu_2(A_1)$	99 (119)	95 (87)	97 (83)	98 (131)	95 (97)	97 (94)		99 (65)		102 (5)
$\nu_3(E)$	259 (41)	241 (25)	249 (26)	246 (48)	234 (25)	240 (26)		227 (25)		232 (42)
$\nu_4(E)$	70 (80)	66 (48)	67 (48)	70 (89)	67 (51)	68 (52)		80 (39)		
					$SeCl_2$[d]					
$\nu_1(A_1)$	443 (100)	427 (100)	437 (100)	424 (100)	417 (100)	426 (100)	415			
$\nu_2(A_1)$	165 (34)	159 (34)	162 (33)	166 (40)	159 (40)	162 (39)	153			
$\nu_3(B_2)$	427 (50)	406 (41)	416 (42)	410 (65)	395 (51)	405 (53)	377			
					$SeBr_2$[e]					
$\nu_1(A_1)$	316 (100)	303 (100)	310 (100)	306 (100)	300 (100)	306 (100)				266
$\nu_2(A_1)$	107 (42)	103 (41)	105 (39)	107 (50)	103 (48)	105 (46)				96
$\nu_3(B_2)$	316 (47)	298 (36)	306 (38)	308 (61)	295 (44)	302 (46)				290
					SeI_2					
$\nu_1(A_1)$	252 (100)	242 (100)	247 (100)	243 (100)	235 (100)	240 (100)				
$\nu_2(A_1)$	78 (73)	75 (66)	76 (63)	78 (67)	75 (63)	76 (60)				
$\nu_3(B_2)$	262 (57)	246 (38)	253 (41)	253 (61)	238 (37)	246 (40)				

[a] For experimental Raman spectra, see ref 8a. [b] For experimental Raman spectra, see ref 8c. [c] This work. [d] For experimental Raman spectra, see ref 29c. [e] For experimental Raman spectra, see ref 29b.

The ESP charges[44] of selenium using the PBE0/cc-pVTZ optimized geometries of the $SeCl_3^+$, $SeBr_3^+$, and SeI_3^+ cations are 0.56, 0.40, and 0.22 e^-. The charge on the selenium atoms expectedly diminishes, as the halogen becomes heavier indicating the increasing delocalization of the cationic charge. They can be compared to those calculated from the cation−anion close contacts[7,8] by use of Brown methodology.[45] The charges from the Brown valency units show the values of 0.45, 0.44, and 0.22 e^- for $SeCl_3^+$, $SeBr_3^+$, and SeI_3^+, respectively.[7,8a] We note that there is a good agreement between the trend of the ESP charges and that calculated from the Brown valency units.

The Solid State and Solution FT-Raman Spectra of $(SeI_3)[AsF_6]$. The solid-state Raman spectrum of $(SeI_3)[AsF_6]$ (see Figure 1) and the Raman frequencies in solution are reported for the first time. The SeI_3^+ frequencies are assigned by comparing them with the computed normal modes given in Table 2. They are also consistent with the assignments that have been carried out previously for $SeCl_3^+$ and $SeBr_3^+$.[7,8c] Small amounts of elemental iodine (a weak signal at 180 cm^{-1};[46] see Figure 1) can be observed in the spectrum of $(SeI_3)[AsF_6]$, but no traces of homopolyatomic iodine cations[47] were detected. Raman frequencies of AsF_6^- were found at 670 (11) cm^{-1}(A_{1g}), 556 (4) cm^{-1} (E_g), 697 (1) cm^{-1} (T_{1u}) and 366 (6) cm^{-1} (T_{2g}).

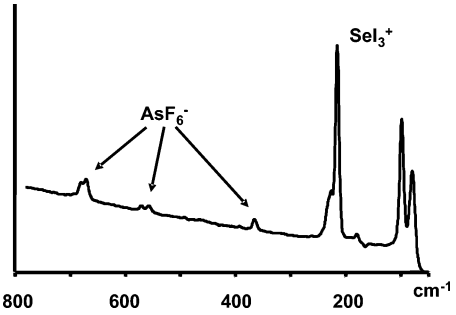

Figure 1. Solid-state FT-Raman spectrum of $(SeI_3)[AsF_6]$.

Computed Vibrational Frequencies. Unscaled calculated vibrational frequencies of SeX_3^+ and SeX_2 (X = Cl, Br, I) at all levels of theory are presented in Table 2. It can be seen that all methods yield values that are close to the experimental values. Standard deviations of different methods vary between 12.0 and 25.9 cm^{-1}. This is an excellent agreement, since neither solvent effects nor corrections for anharmonicity have been considered in these calculations. The largest deviation between the calculated and experimental frequencies is found for the symmetric stretching mode of $SeBr_2$, which is overestimated by 34−50 cm^{-1}.

(44) (a) Singh, U. C.; Kollman, P. A. *J. Comput. Chem.* **1984**, *5*, 129. (b) Breneman, C. M.; Wiberg, K. B. *J. Comput. Chem.* **1990**, *11*, 361.
(45) Brown, I. D. In *Structure and Bonding in Crystals*; O'Keefe, M., Navrotsky, A., Eds.; Academic Press: London, 1981; Vol. 2, p 1.
(46) Nakamoto, K. *Infrared and Raman Spectra of Inorganic and Coordination Compounds*, 4th ed.; John Wiley & Sons, Inc.: New York, 1986.
(47) Brownridge, S. Ph.D. Thesis, University of New Brunswick, Fredericton, New Brunswick, 2001.

This discrepancy is probably due to the solvent effects observed in the experimental Raman spectrum of $SeBr_2$ in thf solution.[2]

The neglect of corrections for anharmonicity and the use of incomplete basis sets is expected to result in the overestimation of experimental fundamentals by the calculations.[48a] This trend is clearly observed for the stretching vibrations that are predicted to lie at too high wavenumbers by most calculations. There is a better agreement between calculated and observed bending modes. However, this better agreement is probably due to fortuitous error compensation, since all computational methods predicted the bond angles to be too large. The calculated normal modes closest to the experimental normal modes were produced with the B3PW91/6-311G(d) method. This and the better overall performance of the smaller 6-311G(d) basis set over the cc-pVTZ basis set in reproducing the observed frequencies is also a consequence of the error compensation, since both the bond lengths and bond angles predicted by the B3PW91/6-311G(d) calculations are longer than the experimental values, and too small wavenumbers would therefore be expected in the frequency calculations involving these geometries.

The agreement between observed and calculated normal modes could be improved by applying scaling factors for calculated frequencies. Several scaling factors for different methods and basis set combinations have been reported in the literature.[48] However, since the scaling factors are based on comparisons of calculated frequencies with experimental data and not readily available for all calculation methods and species, it is better to use unscaled frequencies that are close enough with the experimental values to enable the assignment of known vibrational spectra and the prediction of fundamental vibrations for unknown species.

While no experimental frequencies have been reported for SeI_2,[1] the present calculations can be utilized in their prediction. The calculated fundamental vibrations are 235−252 cm^{-1} (ν_1), 75−78 cm^{-1} (ν_2), and 238−262 cm^{-1} (ν_3) at different levels of theory (see Table 2). Taking into consideration that the stretching modes are likely to be slightly overestimated by the calculations, it is interesting to note that the lowest value for the symmetric Se−I stretching vibration coincides with a strong band at 235 cm^{-1} in the spectrum of solid Se/I_2 eutectic that is assigned to the Se−Se stretch in hexagonal selenium.[5] This would suggest that the evidence of the possible formation of SeI_2 in the solid phase is obscured in the Raman spectrum by an intensive peak due to hexagonal selenium.

The calculated Raman intensities and the experimental solution Raman spectra are compared in Figure 2 for the SeX_3^+ (X = Cl, Br, I) cations. Since both DFT methods yield comparable intensities, only PBE0 results have been shown in Figure 2. Both calculated and experimental Raman intensities of all species have been normalized to that of the fully symmetric ν_1 mode. It can be seen from Figure 2 that the relative intensities of the stretching modes are well reproduced at all levels of theory. By contrast, those of the bending modes are slightly underestimated for $SeCl_3^+$ and $SeBr_3^+$ and overestimated for SeI_3^+. Figure 2 illustrates well the shift of the calculated stretching modes to higher frequencies with cc-pVTZ basis set. MP2 results are more affected by the change of basis set than DFT results. The best overall consistency between the calculated results and experimental Raman spectra seems to be achieved with DFT/6-311G(d) calculations.

^{77}Se Chemical Shifts. The isotropic shielding tensors of selected selenium compounds have also been calculated with different DFT and MP2 methods. This set of calculation methods was augmented with the ZORA/rPBE/QZ4P method in order to estimate the influence of the relativistic effects on the calculated chemical shifts. While the DFT calculations could be performed for all molecular species considered in this paper, the MP2 calculations were not computationally feasible for the larger species due to their excessive memory requirements. They were therefore carried out only for SeH_2, $SeMe_2$, SeX_3^+ and SeX_2 (X = Cl, I) species. Selected bond parameters of the PBE0 optimized geometries of all these reference compounds have been presented in Table 3. They expectedly show a good agreement with experimental information. PBE0/cc-pVTZ optimized geometries were employed in ZORA calculations.

The observed ^{77}Se chemical shifts of the species considered in this work span a wide range of (−345)−1828 ppm. Calculated chemical shifts have been derived from isotropic shielding tensors by subtracting the shielding of the reference compound.

$$\delta(Se) = -[\sigma(Se) - \sigma(Se)_{SeMe2}]$$

The comparison of experimental and calculated chemical shifts is presented in Table 4. It can be seen that all methods exhibit a reasonable linear correlation between the calculated shielding tensors and experimental chemical shifts (see Table 5). Although the 6-311G(d) calculations yield better correlation coefficients with experimental chemical shifts than the cc-pVTZ calculations, the slope of the line that describes the accuracy of the absolute magnitude of the nuclear shielding is significantly closer to unity in case of the cc-pVTZ calculations. The B3PW91/6-311G(d) chemical shifts show the largest deviations from the experimental values. The PBE0 functional performs slightly better with both basis sets than the B3PW91 functional.

Species involving iodine atoms expectedly exhibit largest deviations from the experimental values at nonrelativistic levels of theory emphasizing the need to include relativistic corrections in calculations when selenium is bonded to heavier atoms. It can be seen that the difference between calculated and experimental chemical shifts becomes larger, as the number of heavy atoms bonded to selenium increases. For SeI_3^+ the deviation is over 500 ppm at the PBE0/cc-pVTZ level of theory prohibiting any reliable predictions for the chemical shifts of selenium−iodine species at nonrelativistic levels. As seen in Table 4, the relativistic

(48) (a) Sinha, P.; Boesch, S. E.; Gu, C.; Wheeler, R. A.; Wilson, A. K. *J. Phys. Chem. A* **2004**, *108*, 9213. (b) Halls, M. D.; Velkovski, J.; Schlegel, H. B. *Theor. Chem. Acc.* **2001**, *105*, 413.

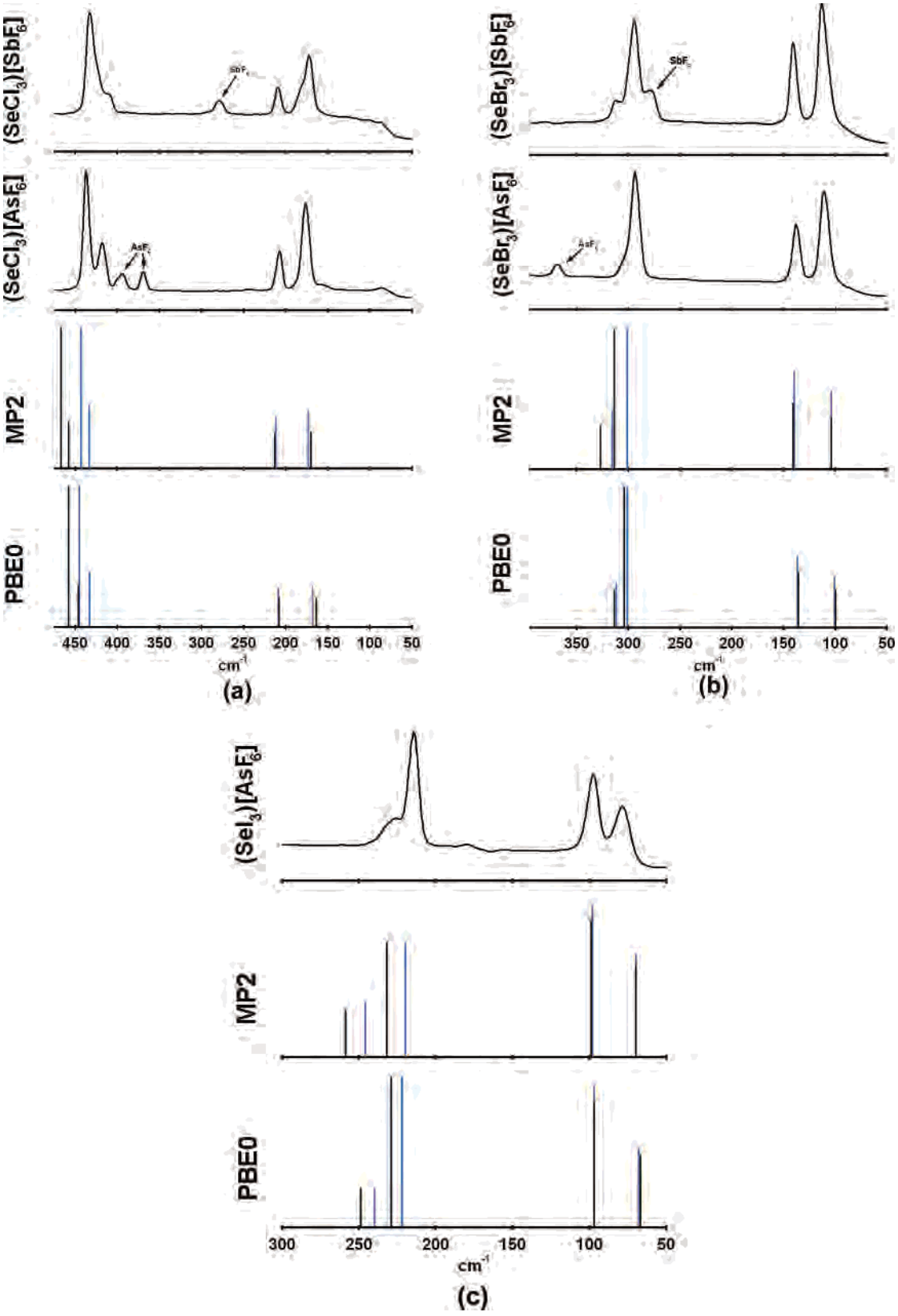

Figure 2. Calculated and experimental solution Raman spectra of $(SeX_3)[MF_6]$ (M = As, Sb). (a) $SeCl_3^+$, (b) $SeBr_3^+$, and (c) SeI_3^+. Uppermost traces represents the observed Raman spectra (For SeI_3^+ only AsF_6^- salt is shown.), the middle trace represents Raman frequencies and intensities at MP2/cc-pVTZ (black trace) and MP2/6-311G(d) (blue trace) levels of theory, and the lowest trace represents the Raman frequencies and intensities at PBE0/cc-pVTZ (black trace) and PBE0/6-311G(d) (blue trace) levels of theory.

ZORA/rPBE/QZ4P calculations improve the agreement for iodine species. However, at the same time the description of the chemical shifts for other species becomes worse. Thus the overall agreement with experimental chemical shifts is not significantly improved by ZORA calculations. This is in line with the usual observation that hybrid functionals

Table 3. PBE0/cc-pVTZ and PBE0/6-311G(d) Optimized Geometries of Some Selenium-Containing Molecules that Have Been Used for the ^{77}Se Chemical Shift Calculations (Q = H or C)

		r(Se-Q)	r(Se−Se)	∠(Q-Se-Q)	∠(Se−Se-Q)	∠(Se−Se−Se)	ref
SeH_2	cc-pVTZ	1.467		91.13			
	6-311G(d)	1.476		90.84			
	exptl	1.460		90.6			49
$SeMe_2$	cc-pVTZ	1.942		97.08			
	6-311G(d)	1.947		96.72			
	exptl	1.943		96.2			50
Se_2Me_2	cc-pVTZ	1.952	2.311		101.13		
	6-311G(d)	1.957	2.323		100.70		
	exptl	1.954	2.326		98.9		51
Se_2Cl_2	cc-pVTZ	2.191	2.232		106.43		
	6-311G(d)	2.216	2.233		106.59		
	exptl	2.203−2.207	2.232		104.0, 104.6		52
Se_2Br_2	cc-pVTZ	2.345	2.240		106.83		
	6-311G(d)	2.359	2.246		107.04		
	exptl	2.357−2.369	2.241−2.257		104.5−107.3		52
Se_2I_2	cc-pVTZ	2.550	2.253		107.27		
	6-311G(d)	2.568	2.265		107.33		
Se_6	cc-pVTZ		2.337			101.46	
	6-311G(d)		2.348			101.47	
	exptl		2.356			101.1	53
Se_8	cc-pVTZ		2.328			106.93	
	6-311G(d)		2.338			106.96	
	exptl		2.325−2.342			103.3−109.1	54c[a]

[a] There are several crystal structure determinations of Se_8.[54] The bond parameters by Foss and Janickis[54c] are presented here as a typical example of a room-temperature structure.

Table 4. Calculated and Observed Chemical Shifts (ppm) of Some Small Selenium Molecules

	MP2/ cc-pVTZ	B3PW91/ cc-pVTZ	PBE0/ cc-pVTZ	MP2/ 6-311G(d)	B3PW91/ 6-311G(d)	PBE0/ 6-311G(d)	ZORA/ rPBE/QZ4P	PBE0/cc-pVTZ + SO term	exptl δ
$SeMe_2$	0	0	0	0	0	0	0	0	0
$SeCl_3^+$	1343	1496	1449	1466	1634	1580	1585	1462	1419[a]
$SeBr_3^+$		1557	1487		1693	1612	1532	1302	1326[b]
SeI_3^+	981	1455	1362	973	1537	1403	1294	935	832[c]
SeH_2	−236	−330	−316	−302	−304	−289	−417	−315	−345[d]
$SeCl_2$	1619	2019	1909	1858	2439	2299	2187	1872	1710−1828[e]
$SeBr_2$		1751	1616		2072	1907	1893	1508	1477−1584[f]
SeI_2	698	1276	1143	664	1231	1053	1023	1007	813[g]
Se_2Me_2		282	259		318	293	304	222	275[h]
Se_2Cl_2		1366	1292		1547	1473	1402	1228	1273[e]
Se_2Br_2		1277	1199		1429	1344	1324	1109	1176[i]
Se_2I_2		1136	1050		1187	1083	1120	947	918[g]
Se_6		684	643		781	735	746	632	685[j]
Se_8		614	575		698	654	646	550	615[j]

[a] Reference 8a. [b] Reference 55. [c] Reference 7. [d] Reference 30. [e] References 2 and 56. [f] References 2, 30a, 56, and 57. [g] Reference 5. [h] Reference 31c. [i] Reference 31b. [j] Reference 31d,e.

Table 5. Linear Relationship between Calculated Shielding Tensors and Experimental Chemical Shifts

	equation: $\sigma_{iso} = A - B \times \delta_{obs}(^{77}Se)$[a]		
method	A	B	corr coeff
B3PW91/cc-pVTZ	1729.9	1.092	−0.9660
PBE0/cc-pVTZ	1785.3	1.036	−0.9704
B3PW91/6-311G(d)	1662.2	1.250	−0.9781
PBE0/6-311G(d)	1731.4	1.183	−0.9834
ZORA/rPBE/QZ4P	1789.3	1.178	−0.9896
PBE0/cc-pVTZ + SO[b]	2011.6	0.993	−0.9924

[a] σ_{iso} is the calculated isotropic shielding tensor and $\delta_{obs}(^{77}Se)$ is the observed chemical shift. [b] SO = the relativistic isotropic spin−orbit shielding tensor from ZORA calculations that has been used as correction term.

generally outperform the gradient corrected functionals in producing chemical properties.[58]

To overcome the problems encountered with the relativistic ZORA/rPBE/QZ4P calculations and at the same time to take into account the spin−orbit-induced relativistic effects that are considered to be the major contributors in the discrepancies between nonrelativistic calculations and experimental chemical shifts, the isotropic spin−orbit shielding tensors from the ZORA calculations have been used as correction

(49) Oka, T.; Morino, Y. *J. Mol. Spectrosc.* **1963**, *10*, 152.
(50) Beecher, J. F. *J. Mol. Spectrosc.* **1966**, *21*, 414.
(51) D'Antonio, P.; Goerge, C.; Lowrey, A. H.; Karle, J. *J. Chem. Phys.* **1971**, *55*, 1071.
(52) Kniep, R.; Korte, L.; Mootz, D. Z. *Naturforsch.* **1983**, *38*, 1.
(53) Miyamoto, Y. *J. Appl. Phys.* **1980**, *19*, 1813.
(54) (a) Cherin, P.; Unger, P. *Acta Crystallogr.* **1972**, *28b*, 313. (b) Burbank, R. D. *Acta Crystallogr.* **1952**, *5*, 236. (c) Foss, O.; Janickis, V. *J. Chem. Soc., Dalton Trans.* **1980**, 624. (d) Maaninen, A.; Konu, J.; Laitinen, R. S.; Chivers, T.; Schatte, G.; Pietikainen, J.; Ahlgren, M. *Inorg. Chem.* **2001**, *40*, 3539.
(55) Murchie, M. P.; Passmore, J.; White, P. S. *Can. J. Chem.* **1987**, *65*, 1584.
(56) Milne, J.; Williams, A. J. *Inorg. Chem.* **1992**, *31*, 4534.
(57) Steudel, R.; Jensen, D.; Baumgart, F. *Polyhedron* **1990**, *9*, 1199.
(58) Koch, W.; Holthausen, M. C. *A Chemist's Guide to Density Functional Theory*, 2nd ed.; Wiley-VHC: Weinheim, 2001.

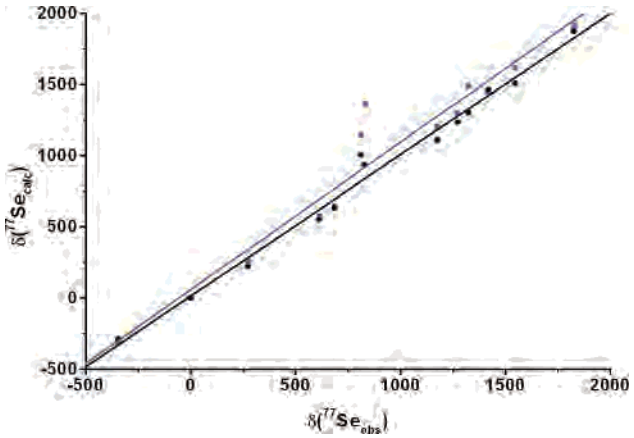

Figure 3. The correlation of calculated chemical shifts with observed chemical shifts of small selenium compounds and the effect of spin−orbit corrections to chemical shifts. Data points marked with ■ represent the best nonrelativistic results calculated at PBE0/cc-pVTZ level of theory, and points marked with • represent the PBE0/cc-pVTZ results with correction terms for spin−orbit effects.

terms for nonrelativistic isotropic shielding tensors calculated at the PBE0/cc-pVTZ level. Although this assumption of the additivity between the PBE0 shieldings and the spin−orbit terms from the ZORA calculation has no firm theoretical ground, Bagno et al.[24c] have successfully obtained the correct order for the ^{13}C chemical shifts in *o*-bromochlorobenzene by adding the ZORA spin−orbit terms to the MP2 shielding tensors. Kaupp et al.[21] have also used separately calculated spin−orbit shielding terms to evaluate the ^{1}H and ^{13}C spin−orbit shifts in some iodo compounds and the ^{31}P shift in tetrahalophosphonium cations.[59] Spin−orbit correction terms seem to improve the agreement between the experimental chemical shifts and the PBE0/cc-pVTZ results yielding the best correlation coefficient and a slope close to unity. The effect of spin−orbit corrections to the ^{77}Se chemical shifts is illustrated in Figure 3. Although the spin−orbit effects are slightly overestimated by the corrections for some of the species with lighter elements, there is a major improvement in the chemical shifts of species involving iodine. The largest deviation from the experimental chemical shifts comes down from 530 to 194 ppm, which significantly improves the potential to apply the calculated chemical shifts in assigning the experimental NMR spectra. The approximation works best for $SeBr_3^+$ and Se_2I_2 species. The calculated chemical shift of Se_2I_2 is only 29 ppm higher than the experimental chemical shift providing further confirmation for the assignment of the chemical shift at 918 ppm [5] to Se_2I_2. The chemical shifts of SeI_2 and SeI_3^+ for which relativistic and spin−orbit effects are more pronounced are still predicted somewhat too large. However, for other species, where only one iodine atom is bonded to the selenium atom, the approximation should produce ^{77}Se chemical shifts in good agreement with the experiment.

The experimental ^{77}Se chemical shift of the $SeCl_2$-containing solution is strongly dependent on the coordinating power of the solvent. In strongly coordinating solvents such as thf and dioxane the ^{77}Se resonance is found at 1828 and 1814 ppm, respectively.[2] In acetonitrile the chemical shift is 1773−1784 ppm,[2,56] in dichloromethane 1762 ppm,[56] and in carbon tetrachloride 1748 ppm.[56] As the solvent becomes more weakly coordinating, the ^{77}Se chemical shift seems to approach the value of 1710 ppm reported for the liquid equilibrium mixture containing $SeCl_2$, Se_2Cl_2 and $SeCl_4$.[1] At the same time, however, the agreement with the computational chemical shift becomes worse.[60] It is also worth noting that the ^{77}Se chemical shift of $SeCl_2$·(tht)$_2$ (tht = tetrahydrothiophene) in carbon disulfide is 1275 ppm at 21 °C and 1299 ppm at 0 °C and that of $SeCl_2$·(tmtu) (tmtu = tetramethylthiourea) in CD_2Cl_2 is 1042 ppm at room temperature.[2] In both adducts there is a linear Cl−Se−Cl fragment with long Se−Cl bonds. The square-planar coordination is completed by tht or tmtu. By contrast, the gas-phase C_{2v} symmetry of $SeCl_2$ is retained in $SeCl_2$·$(OPPh_3)_2$ with a closer agreement between the Se−Cl bond lengths.[3] Consequently, this adduct displays a ^{77}Se resonance of 1442 ppm [3] that lies at a lower field compared to the tht and tmtu adducts and approaches that of a free bent molecule.

$SeBr_2$ shows similar behavior. In thf a ^{77}Se NMR resonance at 1584 ppm is observed,[2] while the chemical shift has been reported to lie at 1496 ppm in CS_2[56] and at 1477 ppm in CH_2Cl_2.[57]

Conclusions

The performance of the MP2, B3PW91 and PBE0 calculations for producing the structural and spectroscopic properties of some selected selenium−halogen and related species have been explored. The results were compared with experimental evidence, where available. In particular, the first solid-state FT-Raman spectrum of $(SeI_3)[AsF_6]$ is reported and assigned in this work.

The calculated structural parameters and vibrational frequencies agree closely with the experimental values. The MP2 results show a greater basis set dependency than the DFT results. Structural parameters are expectedly produced at somewhat better accuracy with the larger cc-pVTZ basis set at each level of theory than with the 6-311G(d) basis set. On the other hand, unscaled 6-311G(d) vibrational frequencies seem to yield better agreement with experimental values. It is concluded to be a consequence of fortuitous error compensation. The Raman intensities show a slightly better agreement with experimental intensities in 6-311G(d) calculations than in cc-pVTZ calculations. The deviation of intensities is largest in case of the bending modes.

Calculated GIAO isotropic shielding tensors correctly predict the trends of the experimental chemical shifts of most

(59) Kaupp, M.; Aubauer, C.; Engelhardt, G.; Klapötke, T. M.; Malkina, O. L. *J. Chem. Phys.* **1999**, *110*, 3897.

(60) A preliminary attempt to include bulk solvent effects in the calculated chemical shifts using the polarizable continuum solvation model with the integral equation formalism leads to corrections of the order of 10−40 ppm. The inclusion of bulk solvent effects, however, did not improve the agreement between the computational and experimental chemical shifts. In a recent article Autschbach and Le Guennic[61] have shown for the ^{195}Pt and ^{205}Tl chemical shifts that the explicit inclusion of first solvent shell in addition to bulk solvent effects is needed to properly describe the solvent effects on the chemical shifts. These calculations are beyond the scope of this work.

(61) Autschbach, J.; Le Guennic, B. *Chem. Eur. J.* **2004**, *10*, 2581.

of the small selenium containing molecules at each level of theory. Of the nonrelativistic methods best agreement with the observed ^{77}Se chemical shifts is achieved with the PBE0/cc-pVTZ calculations. For selenium−iodine species the agreement with experiment is significantly reduced at all nonrelativistic levels of theory. Inclusion of the relativistic effects through ZORA formalism improves the agreement for iodine species. However at the same time there is a loss of accuracy for the chemical shifts of the other species. Best overall agreement with experiment is obtained by including the relativistic spin−orbit shielding tensors from ZORA calculations as correction terms for nonrelativistic PBE0/cc-pVTZ isotropic shielding tensors. In light of the present results it appears that DFT calculations with the inclusion of spin−orbit corrections for NMR properties can be used in the assignment and prediction of ^{77}Se chemical shifts also for selenium−iodine species. However, further investigation is still required for better understanding, how the choice of the calculation method and the inclusion of the relativistic effects influences the accuracy of the calculated ^{77}Se chemical shifts. This investigation is currently in progress.

Acknowledgment. Financial support from the Natural Sciences and Engineering Research Council (NSERC) of Canada, the Academy of Finland, and the Ministry of Education in Finland is gratefully acknowledged. We also thank the Finnish Centre of Scientific Computing for allocation of computational resources.

Supporting Information Available: A table of calculated isotropic shielding tensors at different levels of theory, a figure describing the reaction vessel, and four figures showing the Raman spectra of $(SeX_3)[MF_6]$ (X = Cl, Br; M = As, Sb). This material is available free of charge via the Internet at http://pubs.acs.org.

IC048310W